

Error-rate Analysis of OFDM Operating over Mobile Rayleigh Radio Channel under Multiple RF Impairments

Natalia Y. Ermolova¹, Yaning Zou², *Member, IEEE*, Mikko Valkama², *Member, IEEE*, and
Olav Tirkkonen¹, *Member, IEEE*

¹ Department of Communications and Networking, Aalto University, P.O. Box 13000, FI-00076 Aalto, Finland,
e-mail: first name.last name@aalto.fi

² Department of Communications Engineering, Tampere University of Technology, P.O. Box 553, FIN-33101
Tampere, Finland, e-mail: yaning.zou@tut.fi; mikko.e.valkama@tut.fi

Abstract

We investigate the sensitivity of Orthogonal Frequency Division Multiplexing (OFDM) waveforms to the joint distortion effects of various coexisting non-idealities in the implementation of transceiver radio frequency (RF) electronics, combined also with time variations of the multipath radio channel. We report closed-form performance analysis for a general OFDM mobile radio link, which includes amplitude and phase mismatches between the in-phase (I) and quadrature (Q) rails of both transmitting and receiving devices, as well as carrier frequency offset and oscillator phase noise in the receiving device. The performance metric used here is the detector symbol-error rate built on detailed impairment modeling at link level. To cope with the challenge in evaluation of error rates under non-Gaussian joint interference, we propose a semi-analytical technique that provides accurate estimation of the uncoded symbol-error rate for an arbitrary rectangular QAM. The presented method provides a convenient and time-efficient tool that can be used directly in RF circuit and module design and implementation processes, to derive maximum allowable impairment levels such that the link detection error rate is kept at target level. Also the relative impacts of different impairments can be directly addressed and compared using the provided analysis results.

Index Terms

Direct-conversion transceiver, dirty RF, frequency offset, intercarrier interference, I/Q imbalance, mobile radio channel, OFDM, phase noise, Rayleigh fading, symbol error rate.

I. INTRODUCTION

Orthogonal Frequency Division Multiplexing (OFDM) is widely acknowledged as an efficient transmission technique, well suited for current and future high-data rate adaptive communication systems [1]-[2] such as 3GPP long term evolution (LTE) [3]-[4], digital audio and video broadcasting [5]-[6], and wireless local and metropolitan area networks [7]. This is mainly stemming from relatively simple frequency-domain equalization structures and high flexibility in the power and spectrum use, both at radio link and system levels. With a specially designed cyclic prefix (CP) of a sufficient length, OFDM, based on discrete Fourier transform (DFT) and its inverse (IDFT), completely removes the effect of the delay spread in time-invariant radio channels, and simple one-tap equalization per subcarrier is feasible. In time-selective channels, however, OFDM suffers from inter-carrier interference (ICI) between subcarriers [8]-[9]. There are also several challenging aspects of practical deployment of OFDM related to imperfections in implementations of the radio frequency (RF) analog front-ends (dirty RF effects [10]), stemming from the unavoidable physical limitations of the used electronics [11]-[12], especially in highly-integrated circuit structures. Various RF impairments, such as the in-phase/quadrature (I/Q) imbalance, oscillator phase noise (PN), and carrier frequency offset (CFO), can severely degrade the performance of the OFDM radio link (see, e.g. [10]-[19]). In the existing literature, however, studies of such RF impairments and effects of the fading mobile radio channel, are typically addressed separately. Since in practice these impairments coexist, their joint effect is of great interest. Some works in this area available in the literature present techniques for mitigation of multiple RF impairments and/or for their analysis, see, for example, [20]-[26]. It is worth noting that the theoretical analysis of the joint RF impairments has been the mainly restricted to evaluation of the signal-to-joint interference power ratio, see, for example [21]-[25] and references therein. Error rates, one of the most important metrics in link performance analysis, are evaluated either numerically (using extensive computer simulations) or analytically under the simplifying assumption that the joint interference is Gaussian [19]. Meanwhile, it is widely recognized that the ICI distribution is non-Gaussian [8], [27]. This fact results from violating Lindebergs conditions of the central limit theorem [28] since the ICI power contributed by an individual subcarrier into the joint ICI power of another subcarrier is essentially defined by the distance between the subcarriers [8]. As a result, the Gaussian approximation simplifies the analysis but severely underestimates the bit-error probability as shown in [27]. In addition, the oscillator phase noise, which is an

important imperfection in OFDM receivers [10], [13], is neglected in [19], and the I/Q imbalances are assumed to be frequency-independent, which is not the case in wideband radio context [16]-[17], [29].

The main contribution of this paper is presentation of a semi-analytical method for error-rate evaluation of OFDM with dirty RF operating over the time-frequency-selective Rayleigh channel. An essential feature of the presented technique is taking into account a non-Gaussian structure of joint interference. The method is convenient in a practical use since it allows to avoid lengthy time-consuming computer simulations. Several important RF impairments, such as the transmitter (Tx) and receiver (Rx) frequency-selective I/Q imbalances, Rx oscillator phase noise and CFO are taken into account. The direct-conversion radio topology is assumed for individual transceiver implementations. First, we develop a comprehensive signal model for the radio link under all considered RF imperfections. Based on this model, we then propose a semi-analytical technique for evaluating symbol error rate (SER) of the OFDM radio link assuming an arbitrary rectangular quadrature-amplitude modulated (QAM) alphabet as the subcarrier modulation type. The validity and application of the presented technique are demonstrated via practical examples and computer simulations. In general, the derived results form a framework for radio system and circuit designers, allowing evaluation of the effects of most important RF impairments in the context of OFDM transmission over the double-selective Rayleigh channels. The obtained results can be applied, for example, for derivation of maximum tolerable RF impairment levels satisfying given link performance specifications. Such tool is of great interest for RF circuit design and implementation specialists and greatly helps also the interaction and interplay of RF designers and baseband designers of, e.g., complete wireless modem chips.

The organization of the paper is as follows. The essential RF impairment and radio link models are presented first in Section II. Then in Section III, we present the technique for the SER evaluation. Section IV presents the computer simulation results and illustrations, and conclusions are finally drawn in Section V. Some detailed derivations are then available in Appendix.

II. OFDM RADIO LINK MODELING UNDER TIME-VARIANT MULTIPATH RADIO CHANNEL AND TYPICAL RF IMPAIRMENTS

A. *Mathematical Notations and Preliminaries*

Throughout the text, unless otherwise mentioned, all signals are assumed to be complex-valued, wide-sense stationary random processes with zero mean. The I/Q notation $x = x_I + jx_Q$ is commonly employed for any complex-valued quantity x , where x_I and x_Q denote the corresponding real and imaginary parts. Statistical expectation and complex-conjugation are denoted by $E\{\cdot\}$ and $(\cdot)^*$, respectively. We also

assume that the complex Gaussian random signals and random quantities at hand, under the perfect I/Q balance, are circular, which means that the I and Q components are uncorrelated and have equal variances [30]. For a circular random value $x(n)$, this implies that $E\{x^2(n)\} = 0$. Convolution between two sequences is denoted by \otimes , and the unit discrete impulse function is denoted by $\delta(n)$.

B. Principal Component Models for Characterizing RF Impairments

In this sub-Section, we briefly discuss time- and frequency-domain signal models for characterizing the Tx/Rx I/Q imbalances, phase noise and carrier frequency offset, as well as their impacts in the OFDM waveform context.

1) *I/Q imbalance*: In general, the I/Q imbalance results from unavoidable amplitude and phase mismatches between the transceiver I and Q signal branches caused by relative differences between analog components of the I/Q front-end [11]-[12], [16]-[17]. On the transmitter side, this includes the actual I/Q up-conversion stage as well as the I- and Q-branch digital-to-analog converters and low-pass filters. On the receiver side, the I/Q down-conversion as well as the I and Q branch filtering, amplification, sampling and analog-to-digital stages contribute to the effective I/Q imbalance. In the wideband system context, the overall effective I/Q imbalances vary as a function of the frequency within the system band [11], [16]- [17]. In discrete-time baseband equivalent modeling (see e.g. [16]-[17] and references therein), with $z(n) = z_I(n) + jz_Q(n)$ denoting the perfectly I/Q balanced signal, the realistic frequency-selective I/Q imbalance models appear as

$$z_{\text{Tx(Rx)I/Q}}(n) = \left[g_{1,\text{Tx(Rx)}} \otimes z \right](n) + \left[g_{2,\text{Tx(Rx)}} \otimes z^* \right](n) \quad (1)$$

where $g_{1(2),\text{Tx(Rx)}}$ are the impulse responses of the filters characterizing the Tx(Rx) I/Q imbalances: $g_{1,\text{Tx(Rx)}} = \left[\delta(n) + h_{\text{Tx(Rx)}}(n)g_{\text{Tx(Rx)}}e^{j\varphi_{\text{Tx}}(-\varphi_{\text{Rx}})} \right] / 2$ and $g_{2,\text{Tx(Rx)}} = \left[\delta(n) - h_{\text{Tx(Rx)}}(n)g_{\text{Tx(Rx)}} \times e^{j\varphi_{\text{Tx}}(\varphi_{\text{Rx}})} \right] / 2$, where the filters $h_{\text{Tx(Rx)}}(n)$ represent the I and Q branch *frequency-response differences*, in the transmitter (receiver), while $\{g_{\text{Tx(Rx)}}, \varphi_{\text{Tx(Rx)}}\}$ represent the amplitude and phase imbalances of the Tx (Rx) quadrature mixing stages, respectively [16]-[17].

The transformations (1) interpreted within one OFDM symbol in the frequency-domain (FD) and under a sufficient CP length, correspond to mirror-frequency interference written at the m -th subcarrier as

$$Z_{\text{Tx(Rx)I/Q}}(m) = \gamma_{1,\text{Tx(Rx)}}(m)Z(m) + \gamma_{2,\text{Tx(Rx)}}(m)Z^*(m_{\text{mir}}) \quad (2)$$

where $Z(m)$ represents the data symbol at the m -th subcarrier, $\gamma_{1(2)\text{Tx(Rx)}}$ are the samples of the frequency responses of the filters characterizing the Tx(Rx) I/Q imbalances, and m_{mir} refers to the

mirror frequency of the subcarrier defined as

$$m_{\text{mir}} = \begin{cases} m, & m = 0 \\ N - m - 1, & \text{otherwise} \end{cases} \quad (3)$$

where N denotes the DFT size.

2) *Phase Noise*: In theory, an ideal oscillator generates a pure sine or cosine wave. In practice, however, due to short-term instabilities of practical oscillators, the instantaneous phase is always contaminated by short-term random fluctuations, which result in the so-called phase noise problem [11]-[13]. The impact of transmitter (receiver) phase noise on the signal can be written as [13]

$$z_{\text{Tx(Rx),PN}}(n) = z(n)e^{j\Phi_{\text{Tx(Rx)}}(n)} \quad (4)$$

where $\Phi_{\text{Tx(Rx)}}$ denote the sampled Tx (Rx) oscillator phase noise processes, which are random sequences whose detailed statistics depend on the used oscillator type (free-running (FR) oscillator or phase locked-loop (PLL) based oscillator [13]).

In the OFDM waveform context, PN directly results in ICI since it appears in multiplicative form in (4) [13]. Furthermore, Tx phase noise generally destroys the circular structure of the OFDM symbol. This fact results in additional ICI even if the CP length is enough to capture all delays caused by the system filters. An analysis of Tx PN is a complex separate problem (see [31] and the references therein), and including a general Tx PN into consideration would make the obtained analytical results much less tractable. It was proven, however, in [31, Theorem 2] that the OFDM system with the transmitter and receiver PN is equivalent to that with only receiver PN if the level of transmitter PN is reasonably low, and the radio channel is relatively slow-fading. To simplify the notations and presentation, we follow this approach and refer system PN to the receiver side only. Thus, the FD symbol distorted by PN can be represented as

$$Z_{\text{Rx,PN}}(m) = \frac{1}{N} \sum_{l=0}^{N-1} Z(l)J(m-l) \quad (5)$$

where $J(k) = \sum_{i=0}^{N-1} e^{j\Phi(i)-j2\pi ik/N}$ and $\Phi(i) = \Phi_{\text{Rx}}(i)$.

3) *Carrier Frequency Offset*: In addition to phase noise, stemming from frequency instability of the used oscillator as well as from possible Doppler shift, the carrier frequency offset (CFO) is widely acknowledged as a critical performance limiting factor in OFDM radio links [14]. The frequency offset between the received signal and the Rx oscillator makes the ideal received signal at the detector input to rotate as

$$z_{\text{CFO}}(n) = z(n)e^{j2\pi\Delta f n T_s} \quad (6)$$

where Δf is the frequency offset, and T_s denotes the sampling interval. The FD representation of (6) is:

$$Z_{\text{CFO}}(m) = \frac{1}{N} \sum_{l=0}^{N-1} \sum_{i=0}^{N-1} Z(l) e^{j2\pi\Delta f T_s i - j2\pi(m-l)i/N} = \frac{1}{N} \sum_{l=0}^{N-1} \sum_{i=0}^{N-1} Z(l) e^{j2\pi(\epsilon - m + l)i/N} \quad (7)$$

where $\epsilon = \Delta f T_s N$ denotes the normalized CFO. Clearly, as the I/Q imbalance and PN, the CFO also produces ICI. The signal distorted by both PN and CFO [that is a result of application of (6) to (4)] we denote in the forthcoming derivations with the subscript (PN+CFO).

C. Overall OFDM Radio Link Model under RF Impairments

In this sub-Section, we develop an overall model for the OFDM radio link incorporating the above RF impairment models and effects of the time-varying multipath Rayleigh channel. The block-diagram of the considered system is shown in Fig. 1.

Let $X(m)$ represent the m -th subcarrier transmitted data symbol, and $x(n) = \frac{1}{N} \sum_{m=0}^{N-1} X(m) \times e^{j2\pi mn/N}$ are the time-domain samples of the transmit signal, $m, n = 0, 1, \dots, N-1$. Then the samples of the signal after passing through the time-varying channel with the discrete impulse response $h(n, k)$ (with n and k representing the time and multipath delay, respectively), are

$$r(n) = [h \otimes (g_{1,\text{Tx}} \otimes x + g_{2,\text{Tx}} \otimes x^*)](n) + w(n) \quad (8)$$

where $w(n)$ are the samples of additive channel noise.

After the Rx direct I/Q down-conversion, the signal is contaminated by the CFO, oscillator PN, and the frequencyselective Rx I/Q imbalance. Finally we observe the distorted discrete signal r_d given by

$$r_d(n) = [r_{\text{PN+CFO}} \otimes g_{1,\text{Rx}}](n) + [r_{\text{PN+CFO}}^* \otimes g_{2,\text{Rx}}](n). \quad (9)$$

We introduce the time (n)-dependent frequency (m) response of the double-selective radio channel $H(n, m)$ (i.e. the DFT of $h(n, k)$ w.r.t. k) and define a factor characterizing the contribution of the m -th subcarrier into joint interference (caused by the time variations of the radio channel and frequency offset) at the m_0 -th subcarrier as

$$S_{m,m_0} = \frac{1}{N} \sum_{n=0}^{N-1} H(n, m) e^{j \frac{2\pi(m-m_0+\epsilon)n}{N}}. \quad (10)$$

Assuming that the length of the CP is enough to capture all delays caused by the system filters, taking into account (2), (5), and (7), and separating the useful signal and interference, we obtain a FD representation of the distorted signal in (9) as

$$R_d(m_0) = \underbrace{\left[\alpha_1(m_0) + \alpha_2(m_0) \right]}_{\alpha(m_0)} X(m_0) + \underbrace{\left[\beta_1(m_0) + \beta_2(m_0) \right]}_{\beta(m_0)} X^*(m_0) + ICI(m_0) + N(m_0) \quad (11)$$

where

$$\begin{aligned}
\alpha_1(m_0) &= \frac{\gamma_{1,\text{Rx}}(m_0)\gamma_{1,\text{Tx}}(m_0)}{N} \sum_{l=0}^{N-1} S_{l,m_0} J(m_0 - l), \\
\alpha_2(m_0) &= \frac{\gamma_{2,\text{Rx}}(m_0)\gamma_{2,\text{Tx}}^*(m_{0,\text{mir}})}{N} \sum_{l=0}^{N-1} S_{l,m_{0,\text{mir}}}^* J^*(m_{0,\text{mir}} - l), \\
\beta_1(m_0) &= \frac{\gamma_{1,\text{Rx}}(m_0)\gamma_{2,\text{Tx}}(m_{0,\text{mir}})}{N} \sum_{l=0}^{N-1} S_{l,m_{0,\text{mir}}} J(m_0 - l), \\
\beta_2(m_0) &= \frac{\gamma_{2,\text{Rx}}(m_0)\gamma_{1,\text{Tx}}^*(m_0)}{N} \sum_{l=0}^{N-1} S_{l,m_0}^* J^*(m_{0,\text{mir}} - l),
\end{aligned} \tag{12}$$

$$\begin{aligned}
ICI(m_0) &= \frac{\gamma_{1,\text{Rx}}(m_0)}{N} \sum_{\substack{m=0 \\ m \neq m_0}}^{N-1} \gamma_{1,\text{Tx}}(m) X(m) \sum_{l=0}^{N-1} S_{l,m} J(m_0 - l) \\
&+ \frac{\gamma_{1,\text{Rx}}(m_0)}{N} \sum_{\substack{m=0 \\ m \neq m_0}}^{N-1} \gamma_{2,\text{Tx}}(m_{\text{mir}}) X^*(m) \sum_{l=0}^{N-1} S_{l,m_{\text{mir}}} J(m_0 - l) \\
&+ \frac{\gamma_{2,\text{Rx}}(m_0)}{N} \sum_{\substack{m=0 \\ m \neq m_0}}^{N-1} \gamma_{1,\text{Tx}}^*(m) X^*(m) \sum_{l=0}^{N-1} S_{l,m}^* J^*(m_{0,\text{mir}} - l) \\
&+ \frac{\gamma_{2,\text{Rx}}(m_0)}{N} \sum_{\substack{m=0 \\ m \neq m_0}}^{N-1} \gamma_{2,\text{Tx}}^*(m_{\text{mir}}) X(m) \sum_{l=0}^{N-1} S_{l,m_{\text{mir}}}^* J(m_{0,\text{mir}} - l),
\end{aligned} \tag{13}$$

and

$$N(m_0) = \gamma_{1,\text{Rx}}(m_0) \sum_{l=0}^{N-1} W(l) J(m_0 - l) + \gamma_{2,\text{Tx}}(m_0) \sum_{l=0}^{N-1} W^*(l) J^*(m_{0,\text{mir}} - l) \tag{14}$$

where $W(l)$ is FD channel noise.

Expression (11) represents the symbol distorted by the transmitter-receiver frequency-selective I/Q imbalances, receiver phase noise, and the effects of the mobile radio channel with frequency offsets. In addition to ICI, the formula indicates self-interference between the transmitted symbol and its conjugate, i.e. a frequency-domain I/Q imbalance. This phenomenon was first recognized in [21]. It is observed only if ICI is caused by multiple reasons, such as the I/Q imbalance, Doppler effect and phase noise. In the following Section, this principal received FD signal model is used for detailed link-level performance analysis.

III. OFDM RADIO LINK PERFORMANCE ANALYSIS UNDER MULTIPLE RF IMPAIRMENTS

A. Basic Assumptions and Signal at Detector Input

We assume that the transmitted symbols $X(m)$ are drawn from an $M_I \times M_Q$ - QAM constellation, which is obtained by the combination of two independent pulse-amplitude modulation (PAM) constellations, M_I -ary PAM and M_Q - ary PAM, and d_I and $d_Q = \chi d_I$ are the respective in-phase and quadrature decision distances (i.e. the halves of the distances between the neighboring constellation points).

Concerning the powers of the useful components and ICI in (11) we can first note the following. In practice, the values of the I/Q imbalance coefficients $\gamma_{2,\text{Tx}}$ and $\gamma_{2,\text{Rx}}$ are generally much smaller than the values of $\gamma_{1,\text{Tx}}$ and $\gamma_{1,\text{Rx}}$. The relation between $\gamma_{1,\text{Tx(Rx)}}$ and $\gamma_{2,\text{Tx(Rx)}}$ is generally characterized by the so-called image rejection ratio (IRR) that is expressed as $\left[\frac{\gamma_{1,\text{Tx(Rx)}}}{\gamma_{2,\text{Tx(Rx)}}} \right]$. In modern communication systems, the IRR without digital calibration is about 25-40 dB [32]. Due to this fact, the power of α_1 is much larger than those of α_2 , β_1 , and β_2 even for the worst scenario where the IRR=25 dB (see (12)). Thus, we can approximate the received distorted FD signal model in (11) as

$$R_d(m_0) \approx \alpha_1(m_0)X(m_0) + \overline{ICI}(m_0) + N(m_0) \quad (15)$$

where $\overline{ICI}(m_0)$ is composed of three first components in (13). In terms of d_I this can be written as

$$\begin{aligned} ICI(m_0) &\approx \overline{ICI}(m_0) \\ &= d_I \frac{\gamma_{1,\text{Rx}}(m_0)}{N} \underbrace{\sum_{\substack{m=0 \\ m \neq m_0}}^{N-1} \sum_{l=0}^{N-1} [\gamma_{1,\text{Tx}}(m)A(m)S_{l,m} + \gamma_{2,\text{Tx}}(m_{\text{mir}})A^*(m)S_{l,m_{\text{mir}}}] J(m_0 - l)}_{ICI_1} \\ &\quad + d_I \frac{\gamma_{2,\text{Rx}}(m_0)}{N} \underbrace{\sum_{\substack{m=0 \\ m \neq m_0}}^{N-1} \gamma_{1,\text{Tx}}^*(m)A^*(m) \sum_{l=0}^{N-1} S_{l,m}^* J^*(m_{0_{\text{mir}}} - l)}_{ICI_2} \end{aligned} \quad (16)$$

where $A(l) = A_I(l) + j\chi A_Q(l)$ are the normalized transmitted symbols, (i.e. the transmitted symbol $X(l) = d_I A(l)$), $A_I(l) = [2k_I(l) - 1 - M_I]$, $A_Q(l) = [2k_Q(l) - 1 - M_Q]$, $k_I(l)$ and $k_Q(l)$ take on values from $\{1, 2, \dots, M_I\}$ and $\{1, 2, \dots, M_Q\}$, respectively.

It is seen from (16) that $\overline{ICI}(m_0)$ conditioned on the normalized transmitted symbols $\mathbf{A} = \{A(l)\}$ and PN samples, is complex zero-mean Gaussian. Eqs. (10) and (12) then indicate that also $\alpha_1(m_0)$ is complex zero-mean Gaussian when conditioned on the PN samples. Note, however, that generally $\overline{ICI}(m_0)$ depends on $\alpha_1(m_0)$.

The following lemma can be easily proved.

Lemma: If Z and Y are zero-mean Gaussian and arbitrarily correlated then

$$Z = \rho Y + \eta \quad (17)$$

where $\rho = \frac{E\{ZY^*\}}{\sigma_Y^2}$, σ_Y^2 is the variance of Y , η is zero-mean Gaussian, and Y and η are uncorrelated.

Based on Lemma, we can now represent $\overline{ICI}(m_0)$ in (16) (conditioned on \mathbf{A} and the PN samples) as

$$\overline{ICI}(m_0) = \rho(m_0)\alpha_1(m_0) + \eta(m_0) \quad (18)$$

where

$$\rho(m_0) = \frac{E\{\overline{ICI}(m_0)\alpha_1^*(m_0)\}}{\sigma_{\alpha_1(m_0)}^2}, \quad (19)$$

and $\sigma_{\alpha_1(m_0)}^2$ denotes the variance of $\alpha_1(m_0)$ when conditioned on \mathbf{A} and the PN samples. Closed-form expression for this variance is evaluated in Appendix, eq. (30). Then (15) can be re-written as

$$R_d(m_0) \approx \alpha_1(m_0) [X(m_0) + \rho(m_0)] + \eta(m_0) + N(m_0). \quad (20)$$

Under the simplest single-tap equalizer, we then obtain from (20) that

$$\tilde{R}_d(m_0) = R_d(m_0)/\alpha_1(m_0) \approx X(m_0) + \underbrace{[\eta(m_0) + N(m_0)]/\alpha_1(m_0)}_{\xi(m_0)}. \quad (21)$$

B. Error Probability Analysis

In general, error probability evaluation requires knowledge about the statistical distribution and power of interference in (21). We can now observe the following.

1) When conditioned on the transmitted symbols, PN samples, and $\alpha_1(m_0)$, joint interference $\xi(m_0)$ on the right-hand side (RHS) of (21) is Gaussian.

2) Although $\eta(m_0)$ and $\alpha_1(m_0)$ on the RHS of (21) are uncorrelated and jointly Gaussian, they are generally dependent. Below, we give more details about this phenomenon that may be observed only in the case of complex-valued Gaussian processes where, in contrast to the case of real-valued processes, uncorrelatedness is not equivalent to independence.

It is seen from (10), (13), and (19) that $\alpha_1(m_0)$ depends on both components of ICI, denoted ICI_1 and ICI_2 , in (16) because each of the above quantities depends on the channel gains $H(n, m)$ and on their conjugates $H^*(n, m)$. Considering now the cross-correlation $E\{ICI_1\alpha_1^*(m_0)\}$, we observe that it is composed of terms containing expectations of the form $E\{H(n_1, m_1)H^*(n_2, m_2)\}$, and thus the part of $\eta(m_0)$ in (21) resulting from $ICI_1(m_0)$ in (19) (which we denote as $\eta_1(m_0)$), is independent of $\alpha_1(m_0)$.

This is, however, not the case of $ICI_2(m_0)$ in (16). It is seen that $ICI_2(m_0)$ and $\alpha_1(m_0)$ are uncorrelated since the cross-correlation $E\{ICI_2\alpha_1^*(m_0)\}$ is the sum of the components containing only

expectations of the form $E\{H(n_1, m_1)H(n_2, m_2)\}$, which are zero due to the circularity of $H(n, m)$. At the same time, $ICI_2(m_0)$ and $\alpha_1(m_0)$ are generally dependent since $H(n, m)$ generally does depend on $H^*(n, m)$. Thus the part of $\eta(m_0)$ resulting from $ICI_2(m_0)$ (denoted as $\eta_2(m_0)$) depends on $\alpha_1(m_0)$. It is worth noting that this effect may be negligible for relatively wideband signals with a large number of the subcarriers where for the most of $m_1 \neq m_2$, $H(n_1, m_1)$ is independent of $H(n_2, m_2)$.

In general, we see from (21) that $\xi(m_0)$ conditioned on the PN samples and transmitted symbols \mathbf{A} is complex-valued Gaussian noise with the non-zero mean $\rho(m_0)$ and variance $\sigma_{\xi(m_0)}^2$. Their closed-form evaluation is given in Appendix.

The conditional symbol-error probability over the m_0 -th subcarrier can be expressed as

$$P(m_0) = 1 - (1 - P_I(m_0))(1 - P_Q(m_0)) \quad (22)$$

where $P_I(m_0)$ and $P_Q(m_0)$ are the symbol error probabilities of the in-phase and quadrature components over the m_0 -th subcarrier, respectively. They are defined in a similar manner. A non-zero mean of Gaussian noise in (21) results in non-equal upper and lower decision distances for inner constellation points that are:

$$d_{I_1}(m_0) = d_I + \text{Re}\{\rho(m_0)\} \quad \text{and} \quad d_{I_2}(m_0) = -d_I + \text{Re}\{\rho(m_0)\}. \quad (23)$$

Eq. (23) defines also the quadrature decision distances after changing d_I to d_Q and $\text{Re}\{\cdot\}$ to $\text{Im}\{\cdot\}$.

Since conditional interference in (21) is Gaussian, and errors may occur only in one direction for the edge constellation points, we obtain that the conditional SERs $P_{I(Q)}(m_0)$ are:

$$\begin{aligned} P_{I(Q)}(m_0) &= \frac{M_{I(Q)} - 1}{M_{I(Q)}} \left[Q \left(\frac{|\alpha_1(m_0)| (d_{I(Q)} + \text{Re}(\text{Im})\{\rho(m_0)\})}{\sqrt{2}\sigma_{\xi(m_0)}} \right) \right. \\ &\quad \left. + Q \left(\frac{|\alpha_1(m_0)| (d_{I(Q)} - \text{Re}(\text{Im})\{\rho(m_0)\})}{\sqrt{2}\sigma_{\xi(m_0)}} \right) \right] \\ &\quad \text{if } |\text{Re}(\text{Im})\{\rho(m_0)\}| < d_{I(Q)}, \quad \text{and} \\ P_{I(Q)}(m_0) &= \frac{M_{I(Q)} - 1}{M_{I(Q)}} \left[1 - Q \left(\frac{|\alpha_1(m_0)| (-d_{I(Q)} + 2|\text{Re}(\text{Im})\{\rho(m_0)\})|}{\sqrt{2}\sigma_{\xi(m_0)}} \right) \right. \\ &\quad \left. + Q \left(\frac{|\alpha_1(m_0)| (d_{I(Q)} + 2|\text{Re}(\text{Im})\{\rho(m_0)\})|}{\sqrt{2}\sigma_{\xi(m_0)}} \right) \right] \\ &\quad \text{otherwise.} \end{aligned} \quad (24)$$

It is seen from (22) and (24) that evaluation of the unconditional SER requires first averaging of the Gaussian Q-function and product of two Gaussian Q-functions over the Rayleigh distribution (40)

(see Appendix) and then averaging of the obtained $P(m_0) = SER|_{PN, \mathbf{A}}$ over the samples of PN and data symbols. Averaging over the Rayleigh distribution can be done numerically if the exact effect of the dependence of the power of interference in (21) on $\alpha_1(m_0)$ is taken into account. An approximate analytical solution under this scenario and assuming only the Rx I/Q imbalance and frequency-selective fading, is proposed in [33].

If the interference power in (21) is assumed independent of $\alpha_1(m_0)$, the average over the Rayleigh distribution SER can be evaluated in a closed form. Below we give expressions for evaluation of the above averages using the basic results from [34, vol. 2, eq. (2.8.5.6)] and [35, eq. (5)]. The averaged expression are:

$$\begin{aligned}
E_{w.r.t.|\alpha_1(m_0)|} \{Q(|\alpha_1(m_0)| \cdot p)\} &= 0.5 \left[1 - \left(\frac{p^2 \cdot \sigma_{\alpha_1(m_0)}^2}{2 + p^2 \sigma_{\alpha_1(m_0)}^2} \right)^{1/2} \right], \\
E_{w.r.t.|\alpha_1(m_0)|} \{Q(|\alpha_1(m_0)| \cdot p_1) Q(|\alpha_1(m_0)| \cdot p_2)\} &= \frac{1}{4} - \frac{1}{2\pi} \\
&\times \left[\left(\frac{p_1^2 \cdot \sigma_{\alpha_1(m_0)}^2}{2 + p_1^2 \sigma_{\alpha_1(m_0)}^2} \right)^{1/2} \tan^{-1} \left(\frac{p_2}{p_1} \left(\frac{2 + p_1^2 \sigma_{\alpha_1(m_0)}^2}{p_1^2 \sigma_{\alpha_1(m_0)}^2} \right)^{1/2} \right) \right. \\
&\left. + \left(\frac{p_2^2 \cdot \sigma_{\alpha_1(m_0)}^2}{2 + p_2^2 \sigma_{\alpha_1(m_0)}^2} \right)^{1/2} \tan^{-1} \left(\frac{p_1}{p_2} \left(\frac{2 + p_2^2 \sigma_{\alpha_1(m_0)}^2}{p_2^2 \sigma_{\alpha_1(m_0)}^2} \right)^{1/2} \right) \right]. \tag{25}
\end{aligned}$$

It can be easily shown that the arguments of the Q -functions in (25) are directly expressed in terms of $\frac{d_I^2}{\sigma_W^2}$. In turn, this ratio can be expressed in terms of the transmitted SNR since for rectangular $M_I \times M_Q$ -QAM, the SNR is defined as the ratio of the average symbol energy to the noise power [35], i.e.

$$SNR = \frac{d_I^2}{\sigma_W^2} \cdot \frac{(M_I^2 - 1) + \chi^2(M_Q^2 - 1)}{3}. \tag{26}$$

Thus the arguments of the Q -functions in (25) are expressed explicitly in terms of the transmitted SNR.

The conditional $SER|_{PN, \mathbf{A}}$ derived above must be next averaged over the normalized transmitted symbols \mathbf{A} and samples of PN. This can be done by numerical evaluation if N is not too large. For the arbitrary value of N , the simplest way of obtaining the unconditional SER is the method of Monte Carlo simulations, i.e. L random sequences of the transmitted symbols and samples of PN are generated, and the unconditional SER is expressed as

$$SER(m_0) \approx \frac{1}{L} \sum_{l=0}^{L-1} SER|_{PN, \mathbf{A}}(m_0). \tag{27}$$

Finally, the average SER is obtained by averaging (27) over all subcarriers:

$$SER = \frac{1}{N} \sum_{i=0}^{N-1} SER(i). \tag{28}$$

IV. NUMERIC VERIFICATIONS, ILLUSTRATIONS, AND ANALYSIS

In this Section, we analyze and illustrate the separate and joint impacts of all the considered transceiver RF impairments on link-level performance of OFDM transmission systems using extensive computer simulations. As a practical example, an OFDM transmission link with subcarrier spacing of 15 kHz conforming with the basic 3GPP-LTE specifications [3] is considered. The operating carrier frequency of the used radio electronics is assumed to be 2GHz, and only 16 subcarriers are deployed to form OFDM signal waveforms to simplify the numerical verification simulations. The wireless transmission environment is modeled as a Rayleigh fading multipath channel with the power delay profile of $\{0, 1.85, 1.64\}$ dB at multi-path taps $\{0, 4.17, 8.33\}$ μs respectively, where the corresponding exact fading statistics follows Jakes' model [35], and different mobility values are demonstrated. The channel rms delay is 3.447 μs , and we choose the cyclic prefix of length 14 μs . Thus the total symbol duration T_{sympb} is approximately 81 μs . 16- and 64-QAM are used as subcarrier data modulations for analyzing the detection error rate. In addition to a free-running oscillator, described by its 3dB bandwidth [13], a state-of-the art charge-pump PLL (CPPLL) is implemented. Its phase noise performance is discussed in [13] in more detail, and the power spectrum density of PN at 1MHz offset from the nominal oscillating frequency is assumed to be in the range of -130dBc/Hz to -100dBc/Hz. This represents realistic integrated oscillator phase noise performance on deep-submicron silicon processes. The frequency-selectivity of the I/Q imbalances is modeled by two-tap branch filters with the impulse responses $(1 - C_{\text{bf,Tx}})$ at the transmitter side and $(1 - C_{\text{bf,Rx}})$ at the receiver side, where $C_{\text{bf,Tx}}$ and $C_{\text{bf,Rx}}$ are relatively small values compared to 1, corresponding to a mild frequency-selectivity. The tap spacing is one signal sample.

As a starting point, the impacts of different RF impairments on the OFDM radio link performance are analyzed and compared. Here we especially demonstrate the impact of changing the level of one individual RF impairment and illustrate its impact on the link performance. The used parameter ranges are given in Table 1, where step 1 corresponds to fairly low impairment values, which are then increased gradually in the following steps 2-6. As it is seen from Table 1, we deliberately choose the maximal vehicular velocity (110km/h) such that the radio channel could be considered slow-fading in order to satisfy the conditions of Theorem 2 in [30]. Under this velocity, the maximal Doppler frequency f_m is 203.7 Hz, and thus $f_m T_{\text{sympb}} \approx 0.016 \ll 1$. Hence based on [30, Theorem 2] we refer PN to the receiver side only. The results are illustrated in Fig. 2-3, where also the link performance in the ideal case (no impairments) is depicted for reference as blue dashed lines. The presented simulation results agree well with our analytical derivations. As the obtained results illustrate, the OFDM link performances degrade

gradually when increasing the RF impairment levels, yet the exact performance degradation values vary quite a bit for different impairments. With given system parameters, when a free-running oscillator is used at the receiver side, CFO, phase noise and Rx phase imbalances are shown as the top three contaminating sources. On the other hand, if the CPPLL type oscillator is used at the receiver side, Rx phase noise is not a big issue any more due to much better phase noise characteristics compared to free running oscillator. Dominant RF impairments are then CFO and Rx phase imbalance. Overall, the analysis results clearly demonstrate that even fairly low RF impairment values, when co-existing, can result in severe performance degradation in OFDM radio links. This fact motivates application and development of digitally-assisted RF calibration methods, discussed e.g. in [10]- [12], [16].

Next, the accuracy and validation of the proposed link-level performance analysis are demonstrated using 20 sets of randomly selected yet reasonable impairment parameter values given in Table 2. In Table 3, the average received SNRs, which are used with the 20 impairment parameter sets for performance evaluations, are also given respectively. In more details, the average received SNRs in the range of 25-35dB are assigned with 64QAM subcarrier modulation, while SNRs in the range of 20-30dB are applied with 16QAM subcarrier modulation. With impairment and SNR parameters given in Tables 2-3, the resulting link-level performance degradation due to the presence of multiple impairments is evaluated in terms of SER one by one, using both the proposed analysis and extensive computer simulations. With given parameters here, the simulation time for evaluating error rates using proposed semi-analytic method is in the scale of 1/10 of simulation time for evaluating error rates using traditional numerical full link simulations. Meanwhile, the estimated and simulated link performance in terms of SER versus SNR is compared using parameter set no. 3 given in the Table 2 with both 16 QAM and 64 QAM subcarrier modulations. The results are shown in Fig. 4-7. It is seen that our theoretical estimates agree well with simulation results in all cases considered.

V. CONCLUSION

In this paper, we analyzed the symbol-error rate of OFDM with “dirty RF” problems operating over the double-selective Rayleigh radio channel. The analysis took into account the transmitter and receiver frequency-selective I/Q imbalances, receiver phase noise and carrier frequency offset. First we derived a detailed link model. On this basis, we presented a semi-analytical technique for evaluation of the symbol error rate for the arbitrary rectangular QAM. This is the main contribution of this paper. The proposed method essentially takes into account the non-Gaussian distribution of joint interference and allows to overcome uncertainty caused by its unknown real distribution.

In our analysis we observed new effects that were absent in the conventional OFDM system without multiple RF impairments. One of them was the cross-correlation of the useful component of the distorted signal and ICI caused by the multiple impairments. By separating ICI into the correlated and uncorrelated parts, we showed that conditional (to the transmitted data and PN samples) interference was Gaussian with the non-zero mean. The second phenomenon observed was the dependence of the uncorrelated part of ICI on the useful component. This effect is caused by the receiver I/Q imbalance. Both phenomena were carefully considered and treated.

Our intensive computer simulations of OFDM link performance under multiple RF impairments showed very good agreement with the derived theoretical estimates for a large variety of the parameter combinations. It is important to note that the proposed semi-analytical procedure provides decreasing of the computational time in a common PC approximately in ten times. Hence this technique can be used as an alternative to complex, time-consuming and cumbersome numerical full link simulation-based methods that have been so far the main tool of OFDM analysis under many simultaneously co-existing RF impairments.

APPENDIX

EVALUATION OF INTERFERENCE POWER IN (21)

We start with evaluation of $\rho(m_0)$ defined by (19). The expectation $E \left\{ \overline{ICI} \alpha_1^*(m_0) \right\} = E_1(m_0)$, conditioned on the transmitted symbols and PN samples is given by

$$E_1(m_0) = d_1 \left\{ \frac{|\gamma_{1,\text{Rx}}(m_0)|^2 \gamma_{1,\text{Tx}}^*(m_0)}{N^2} \right. \\ \times \sum_{\substack{m=0 \\ m \neq m_0}}^{N-1} \sum_{l_1, l_2=0}^{N-1} \left[\gamma_{1,\text{Tx}}(m) A(m) E \left\{ S_{l_1, m} S_{l_2, m_0}^* \right\} + \gamma_{2,\text{Tx}}^*(m_{\text{mir}}) A^*(m) E \left\{ S_{l_1, m_{\text{mir}}} S_{l_2, m_0}^* \right\} \right] \\ \left. \times J(m_0 - l_1) J^*(m_0 - l_2) \right\} = d_1 \Xi_1(m_0), \quad (29)$$

and $\sigma_{\alpha_1(m_0)}^2$ is given by

$$\sigma_{\alpha_1(m_0)}^2 = \frac{|\gamma_{1,\text{Rx}}(m_0) \gamma_{1,\text{Tx}}^*(m_0)|^2}{N^2} \sum_{l_1, l_2=0}^{N-1} J(m_0 - l_1) J^*(m_0 - l_2) E \left\{ S_{l_1, m_0} S_{l_2, m_0}^* \right\}. \quad (30)$$

We assume the wide-sense stationary uncorrelated scattered channel, which is a typical assumption in analysis work. Let the impulse response of the radio channel be characterized by Q complex path gains $h_p(t) (p = 0, \dots, Q - 1)$, and the cross-correlation

$$E \left\{ h_p(t) h_q^*(t + \tau) \right\} = E_p \delta(p, q) J_0(2\pi f_m \tau) \quad (31)$$

where E_p is the power of the p th path, $J_0(\cdot)$ is the zero-order Bessel function of the first kind, and $\delta(p, q)$ is the Kronecker delta [8]. Then the expectation $E \{S_{l_1, m_1} S_{l_2, m_2}^*\}$ in (29)-(30) can be evaluated as

$$\begin{aligned} E \{S_{l_1, m_1} S_{l_2, m_2}^*\} &= \frac{1}{N^2} \sum_{n_1, n_2=0}^{N-1} E \{H(n_1, m_1) H^*(n_2, m_2)\} \exp \left[j \frac{2\pi(m_1 - l_1 + \epsilon)n_1}{N} \right] \\ &\times \exp \left[-j \frac{2\pi(m_2 - l_2 + \epsilon)n_2}{N} \right] = \frac{1}{N^2} \sum_{n_1, n_2=0}^{N-1} \exp \left[j \frac{2\pi}{N} (m_1 n_1 - m_2 n_2) \right] \\ &\times \sum_s E \{h_s(n_1) h_s^*(n_2)\} \exp \left[j \frac{2\pi}{N} s(m_1 - m_2) \right] \exp \left[j \frac{2\pi}{N} (\epsilon - l_1)n_1 - (\epsilon - l_2)n_2 \right]. \end{aligned} \quad (32)$$

Assuming next that the CFO and channel gains are independent we obtain that

$$\begin{aligned} E \{S_{l_1, m_1} S_{l_2, m_2}^*\} &= \frac{F(m_1 - m_2)}{N^2} \sum_{n_1, n_2=0}^{N-1} J_0 \left[\frac{2\pi\Delta(n_2 - n_1)}{N} \right] \\ &\times \exp \left\{ j \frac{2\pi}{N} [(m_1 - l_1 + \epsilon)n_1 - (m_2 - l_2 + \epsilon)n_2] \right\} \end{aligned} \quad (33)$$

where $F(g) = \sum_s E_s \exp(-j \frac{2\pi s g}{N})$, $g = -N + 1, \dots, N - 1$, and Δ is the maximal Doppler frequency normalized to the subcarrier spacing. Thus we obtain from (19) and (29)-(33) that $\rho(m_0) = d_1 \frac{\Xi_1(m_0)}{\sigma_{\alpha_1(m_0)}^2}$.

Concerning next the power of interference in (21), we observe that $\sigma_{\xi(m_0)}^2 = \sigma_{\eta(m_0)}^2 + \sigma_N^2$, and the interference term η is the sum of two components η_1 and η_2 resulting from ICI_1 and ICI_2 , respectively [see (16)]. One can show by direct evaluation that $E \{\eta_1 \eta_2^*\} = 0$, and thus $\sigma_{\eta(m_0)}^2 = \sigma_{\eta_1(m_0)}^2 + \sigma_{\eta_2(m_0)}^2 |_{\alpha_1(m_0)}$. It is then seen from (16) that

$$\begin{aligned} \sigma_{\eta_1(m_0)}^2 &= d_1 \frac{|\gamma_{1, \text{Rx}}(m_0)|^2}{N^2} \sum_{\substack{m_1, m_2=0 \\ m_1, m_2 \neq m_0}}^{N-1} \sum_{l_1, l_2=0}^{N-1} E \left\{ \left[\gamma_{1, \text{Tx}}(m_1) A(m_1) S_{l_1, m_1} + \gamma_{2, \text{Tx}}^*(m_{1, \text{mir}}) A^*(m_1) S_{l_1, m_{1, \text{mir}}} \right] \right. \\ &\times \left. \left[\gamma_{1, \text{Tx}}^*(m_2) A^*(m_2) S_{l_2, m_2}^* + \gamma_{2, \text{Tx}}(m_{2, \text{mir}}) A(m_2) S_{l_2, m_{2, \text{mir}}}^* \right] \right\} J(m_0 - l_1) J^*(m_0 - l_2). \end{aligned} \quad (34)$$

The conditional variance $\sigma_{\eta_2(m_0)}^2 |_{\alpha_1(m_0)} = \sigma_{|\eta_2(m_0)|}^2 |_{|\alpha_1(m_0)|}$. Since $\alpha_1(m_0)$ and $\eta_2(m_0)$ are jointly Gaussian, $|\alpha_1(m_0)| = X_1$ and $|\eta_1(m_0)| = X_2$ are subject to the bivariate Rayleigh distribution [36]:

$$p_{X_1, X_2}(x_1, x_2) = \frac{4x_1 x_2}{\sigma_1^2 \sigma_2^2 (1-r)} \exp \left[\frac{-1}{1-r} \left(\frac{x_1^2}{\sigma_1^2} + \frac{x_2^2}{\sigma_2^2} \right) \right] I_0 \left[\frac{2\sqrt{r} x_1 x_2}{(1-r)\sigma_1 \sigma_2} \right] \quad (35)$$

where $\sigma_1^2 = \sigma_{\alpha_1(m_0)}^2$, $\sigma_2^2 = E \{|\eta_1(m_0)|^2\}$, $r = \frac{\text{cov}\{x_1^2, x_2^2\}}{\sigma_1 \sigma_2}$ (where cov denotes covariance) is a correlation coefficient, and $I_0(\cdot)$ is the modified Bessel function of the first kind and zero order.

The variance σ_1^2 is defined by (30), and the variance σ_2^2 in turn is given by

$$\begin{aligned} \sigma_2^2 &= d_1^2 \frac{|\gamma_{2,\text{Rx}}(m_0)|^2}{N^2} \sum_{\substack{m_1, m_2=0 \\ m_1, m_2 \neq m_0}}^{N-1} \gamma_{2,\text{Tx}}^*(m_1) \gamma_{1,\text{Tx}}(m_2) A^*(m_1) A(m_2) \\ &\times \sum_{l_1, l_2=0}^{N-1} E \left\{ S_{l_1, m_1}^* S_{l_2, m_2} \right\} J^*(m_{0,\text{mir}} - l_1) J(m_{0,\text{mir}} - l_2) \end{aligned} \quad (36)$$

where the expectation on the RHS of (36) is defined in (32)-(33). The variances $\text{var} \{x_{1(2)}^2\} = 2\sigma_{1(2)}^4$, and the covariance $\text{cov} \{x_1^2 x_2^2\} = E \{x_1^2 x_2^2\} - E \{x_1^2\} E \{x_2^2\}$ [38]. The expectations $E \{x_1^2\}$ and $E \{x_2^2\}$ are defined in (30) and (36), respectively, and $E \{x_1^2 x_2^2\}$ is:

$$\begin{aligned} E \{x_1^2 x_2^2\} &= d_1^2 \frac{|\gamma_{1,\text{Rx}}(m_0) \gamma_{1,\text{Tx}}(m_0) \gamma_{2,\text{Rx}}(m_0)|^2}{N^{16}} \sum_{l_1, l_2=0}^{N-1} J(m_0 - l_1) J^*(m_0 - l_2) \\ &\times \sum_{m_1, m_2=0}^{N-1} \gamma_{1,\text{Tx}}^*(m_1) \gamma_{1,\text{Tx}}(m_2) A^*(m_1) A(m_2) \sum_{l_3, l_4=0}^{N-1} J^*(m_{0,\text{mir}} - l_3) J(m_{0,\text{mir}} - l_4) \\ &\times E \{H(n_1, l_1) H^*(n_2, l_2) H(n_3, l_3) H^*(n_4, l_4)\} \exp \left\{ j \frac{2\pi}{N} \right. \\ &\times [n_1(l_1 - m_0 + \epsilon) - n_2(l_2 - m_0 + \epsilon) + n_3(l_3 - m_1 + \epsilon) - n_4(l_4 - m_2 + \epsilon)] \left. \right\}. \end{aligned} \quad (37)$$

The expectation in (37) can be evaluated on the basis of Reed's theorem [38]:

$$\begin{aligned} E \{H(n_1, l_1) H^*(n_2, l_2) H(n_3, l_3) H^*(n_4, l_4)\} &= E \{H(n_1, l_1) H^*(n_2, l_2)\} E \{H(n_3, l_3) H^*(n_4, l_4)\} \\ &+ E \{H(n_1, l_1) H^*(n_4, l_4)\} E \{H(n_3, l_3) H^*(n_2, l_2)\} \end{aligned} \quad (38)$$

where the expectations on the RHS of (38) are defined in (32)-(33).

Thus the conditional variance $\sigma_{\eta_2(m_0)|\alpha_1(m_0)}^2$ can be defined as

$$\begin{aligned} \sigma_{\eta_2(m_0)|\alpha_1(m_0)}^2 &= E \left\{ |\eta_2(m_0)|^2 \middle| \alpha_1(m_0) \right\} = \int_0^\infty x_2^2 p_{X_1, X_2}(x_2 | x_1) dx_2 \\ &= \frac{1}{p_{X_1}(x_1)} \int_0^\infty x_2^2 p_{X_1, X_2}(x_1, x_2) dx_2 \end{aligned} \quad (39)$$

where

$$p_{X_1}(x_1) = \frac{2x_1}{\sigma_{\alpha_1(m_0)}^2} \exp \left(-\frac{x_1^2}{\sigma_{\alpha_1(m_0)}^2} \right) \quad (40)$$

is the marginal probability density function of the Rayleigh distribution [38]. Evaluating (39) by using an integration formula [33, vol. 2, 2.15.5.4] and applying then the transformation formula for the Kummer hypergeometric function, ${}_1F_1(a; b; z) = \exp(z) {}_1F_1(b - a; b; -z)$ [33, vol. 3, Section (6.6)], we obtain that

$$E \{x_2^2 | x_1\} = \sigma_2^2 (1 - r) {}_1F_1 \left(-1; 1; \frac{-r}{(1 - r)\sigma_2^2} x_1^2 \right) = \sigma_2^2 (1 - r) + r x_1^2. \quad (41)$$

Thus we obtain that the power of Gaussian interference in (21) is a linear function of $|\alpha_1(m_0)|^2$.

REFERENCES

- [1] R. Tafazolli (Ed.), *Technologies for Wireless Future. Wireless World Research Forum (WWRF)*, Wiley, New York, 2006.
- [2] H.-H. Chen, M. Guizani, and J. F. Huber, Eds., “Multiple access technologies for B3G wireless communications,” *IEEE Commun. Mag.*, vol. 43, no. 2, Feb. 2005.
- [3] 3GPP Technical Specification, TS 36.211 v. 8.3.0. “Physical channels and modulation (release 8),” May 2008.
- [4] H. Holma and A. Toskala, *LTE for UMTS-OFDMA and SC-FDMA Based Radio Access*, Wiley, New York, 2009.
- [5] [ETS 300 401: Radio Broadcasting Systems; Digital Audio Broadcasting (DAB) to Mobile, Portable and Fixed Receivers, ETSI, February 1995.
- [6] DVB document A133: Implementation Guidelines for a Second Generation Digital Terrestrial Television Broadcasting System (DVB-T2), June 2010.
- [7] H. Liu and G. Li, *OFDM-based Broadband Wireless Networks*, Wiley, New York, 2005.
- [8] Y. Li and L. J. Cimini, “Bounds on the interchannel interference of OFDM in time-varying impairments,” *IEEE Trans. Commun.*, vol. 49, no. 3, pp. 401–404, March 2001.
- [9] S. Tomasin, A. Gorokhov, H. Yang, and J.-P. Linnartz, “Iterative interference cancellation and channel estimation for mobile OFDM,” *IEEE Trans. Wireless Commun.*, vol. 4, no. 1, pp. 238–245, Jan. 2005.
- [10] G. Fettweis, M. Lohning, D. Petrovic, M. Windisch, P. Zillmann, and W. Rave, “Dirty RF: A new paradigm,” *Int. J. Wireless Inform. Networks*, vol. 14, no. 2, pp. 133–148, June 2007.
- [11] B. Razavi, *RF Microelectronics.*, Englewood Cliffs, Prentice-Hall, NJ, 1998.
- [12] S. Mirabbasi and K. Martin, “Classical and modern receiver architectures,” *IEEE Commun. Mag.*, vol. 38, no. 11, pp. 132–139, Nov. 2000.
- [13] D. Petrovic, W. Rave, and G. Fettweis, “Effects of phase noise on OFDM systems with and without PLL: Characterization and compensation,” *IEEE Trans. Commun.*, vol. 55, no. 8, pp. 1607–1616, Aug. 2007.
- [14] P. Moose, “A technique for orthogonal frequency division multiplexing frequency offset correction,” *IEEE Trans. Commun.*, vol. 42, no. 10, pp. 2908–2914, Oct. 1994.
- [15] T.M. B. Schmidl and D.C. Cox, “Robust frequency and timing synchronization for OFDM communications,” *IEEE Trans. Commun.*, vol. 45, no. 12, pp. 1613–1621, Dec. 1997.
- [16] M. Valkama, J. Pirskanen, and M. Renfors, “Signal processing challenges for applying software radio principles in future wireless terminals: An overview,” *Int. J. Commun. Syst.*, vol. 15, pp. 741–769, Oct. 2002.
- [17] Y. Zou, “Analysis and compensation of I/Q imbalances in multi-antenna transmission systems,” Ph.D. Thesis, Tampere University of Technology, Dec. 2009.
- [18] Q. Zou, A. Tarighat, and A. H. Sayed, “Joint compensation of IQ imbalance and phase noise in OFDM wireless systems,” *IEEE Trans. Commun.*, vol. 57, no. 2, pp. 404–414, Feb. 2009.
- [19] M. Krondorf and G. Fettweis, “OFDM link performance analysis under various receiver impairments,” *EURASIP J. Wireless Commun. and Network.*, vol. 2008, article ID 145279.
- [20] J. Tubbax, L. Van der Perre, S. Donnay, M. Engels, M. Moonen, and H. De Man, “Joint compensation of IQ imbalance, frequency offset and phase noise in OFDM receivers,” *Europ. Trans. Telecommun.*, vol. 15, pp. 283–292, 2004.
- [21] B. Narasimhan, D. Wang, S. Narayanan, H. Minn, and N. Al-Dhahir, “Digital compensation of frequency-dependent joint Tx/Rx I/Q imbalance in OFDM systems under high mobility,” *IEEE J. Select. Topics Signal Process.*, vol. 3, no. 3, pp. 405–417, June 2009.

- [22] B. Narasimhan, S. Narayanan, H. Minn, and N. Al-Dhahir, "Reduced-Complexity Baseband Compensation of Joint Tx/Rx I/Q Imbalance in Mobile MIMO-OFDM," *IEEE Trans. Wireless Commun.*, vol. 9, no. 5, pp. 1720–1728, May 2010.
- [23] P. Rabiei, W. Namgoong, and N. Al-Dhahir, "Reduced-Complexity Joint Baseband Compensation of Phase Noise and I/Q Imbalance for MIMO-OFDM Systems," *IEEE Trans. Wireless Commun.*, vol. 9, no. 11, pp. 3450–3460, Nov. 2010.
- [24] R. Zhang, E. K. S. Au, and R. S. Cheng, "Impact of CFO, IQ imbalance and phase noise on the system performance in OFDM systems," in Proc. *IEEE Singapore Int. Conf. Commun. Syst.*, Guangzhou, China, Nov. 2008, pp. 1041–1045.
- [25] V. Syrjälä, M. Valkama, Y. Zou, N. N. Tchamov, and J. Rinne, "On OFDM link performance under receiver phase noise with arbitrary spectral shape," in Proc. *IEEE Wireless Commun. and Network. Conf. 2011 (IEEE WCNC11)*, Cancun, Mexico, March 2011.
- [26] T. C. W. Schenk, R. W. van der Hofstad, E. R. Fledderus, and P. F. M. Smulders, "Distribution of the ICI term in phase noise impaired OFDM system," *IEEE Trans. Wireless Commun.*, vol. 6, no. 4, pp. 148–1500, Apr. 2007.
- [27] W. Feller, *An Introduction to Probability Theory and Its Applications*, vol. 2, Wiley, New York, 1971.
- [28] C. Feng Gu, C. Look Law, and W. Wu, "Time-domain IQ imbalance compensation for wideband wireless systems," *IEEE Commun. Lett.*, vol. 14, no. 6, pp. 539–541, June 2010.
- [29] P. J. Schreier and L. L. Scharf, "Second-order analysis of improper complex random vectors and processes," *IEEE Trans. Signal Process.*, vol. 51, no. 3, pp. 714–725, March 2003.
- [30] P. Liu, Y. Bar-Ness, and J. Zhu, "Effects of phase noise at both transmitter and receiver on the performance of OFDM systems," in Proc. *IEEE Conf. Inform. Sciences and Syst.*, Princeton, NJ, pp. 312–316, March 2006.
- [31] B. Razavi, "Design considerations for direct-conversion receivers," *IEEE Trans. Circuits and Syst.-II*, vol. 44, no. 6, June 1997, pp. 428–435.
- [32] Y. Zou, M. Valkama, N. Y. Ermolova, and O. Tirkkonen, "Analytical Performance of OFDM Radio Link Under RX I/Q Imbalance and Frequency-Selective Rayleigh Fading Channel," in Proc. *IEEE Int. Workshop Signal Process. Advances in Wireless Commun. (SPAWC 2011)*, San Francisco, CA, June 2011, pp. 251–255.
- [33] A. P. Prudnikov, Y. A. Brychkov, and O. I. Marichev, *Integrals and Series*, Gordon and Breach Science Publishers, 1986.
- [34] N. Beaulieu, "A useful integral for wireless communication theory and its application to rectangular signaling constellation error rates," *IEEE Trans. Commun.*, vol. 54, no. 5, pp. 802–805, May 2006.
- [35] G. L. Stuber, *Principles of Mobile Communication*, Kluwer Academic Publisher, 2000.
- [36] M. K. Simon and M.-S. Alouni, "A simple single integral representation of the bivariate Rayleigh distribution," *IEEE Commun. Lett.*, vol. 2, no. 5, pp. 128–130, May 1998.
- [37] A. Papoulis, *Probability, Random Variables, and Stochastic Processes*, McGraw Hill, 1984.
- [38] I. S. Reed, "On a moment theorem for complex Gaussian processes," *IRE Trans. Inform. Theory*, vol. 8, no. 3, pp. 194–195, April 1962.

TABLE 1: GRADUAL CHANGES OF IMPAIRMENT PARAMETERS WITHIN SIX STEPS

Step #	Rx GI [%]	Rx PI [°]	Tx GI [%]	Tx PI [°]	Normalized CFO	V [km/h]	CPPLL [dBc/Hz]
1	0.5	0.5	0.5	0.5	0.005	10	-130
2	2.0	2.0	2.0	2.0	0.020	30	-125
3	3.5	3.5	3.5	3.5	0.035	50	-120
4	5.0	5.0	5.0	5.0	0.050	70	-115
5	6.5	6.5	6.5	6.5	0.065	90	-110
6	8.0	8.0	8.0	8.0	0.080	110	-105

TABLE 2: 20 SETS OF IMPAIRMENT PARAMETERS RANDOMLY SELECTED FROM REALISTIC VALUES.

Set #	Rx GI [%]	Rx PI [°]	Rx $C_{bf,Rx}$	Tx GI [%]	Tx PI [°]	Tx $C_{bf,Tx}$	Normalized CFO	Veloc. [km/h]	PN	
									FR [Hz]	CPPLL [dBc/Hz]
1	3	2	0.02	-1	3	0.03	-0.02	24	89	-103
2	4	-3	0.03	-1	-3	0.02	0.04	82	67	-120
3	-1	4	-0.01	3	0	-0.02	0.01	38	10	-124
4	2	5	0.04	3	2	0	0.01	58	70	-112
5	1	-2	0.02	-3	4	0.01	0.05	25	64	-125
6	-4	3	0.02	0	5	-0.04	-0.02	64	69	-100
7	-2	1	-0.03	-1	1	-0.02	0.03	33	17	-115
8	1	-1	0.01	2	-4	-0.02	0.03	69	46	-132
9	-2	2	-0.04	2	-2	0	-0.01	72	33	-123
10	5	-4	0.03	3	-3	0.04	0.01	78	62	-104
11	4	2	-0.02	-2	4	-0.03	-0.03	50	49	-109
12	2	-2	0.03	2	-3	-0.03	-0.05	17	52	-124
13	-3	-1	0.01	2	3	0.03	0	30	26	-120
14	0	-3	0	-4	-3	-0.04	0.03	93	34	-155
15	3	-2	0.04	-4	-5	0.01	0.02	23	23	-130
16	-4	4	-0.01	0	-2	-0.04	-0.04	85	22	-123
17	-1	2	0.02	5	-3	-0.02	0.01	58	69	-124
18	5	-2	0.05	-2	-3	0.03	0	100	62	-121
19	3	5	0.03	1	1	0	0.02	17	60	-104
20	4	-3	0.02	-3	0	-0.04	-0.02	50	23	-110

TABLE 3: 20 SETS OF SNR PARAMETERS RANDOMLY SELECTED FROM REALISTIC VALUES, USED WITH IMPAIRMENT PARAMETERS GIVEN IN TABLE 2 FOR PERFORMANCE EVALUATIONS.

Set # (refer to Table 1)		1	2	3	4	5	6	7	8	9	10
SNR [dB]	16QAM	21	22	29	28	21	26	25	27	27	26
	64QAM	28	26	28	28	25	30	32	32	27	34
Set # (refer to Table 1)		11	12	13	14	15	16	17	18	19	20
SNR [dB]	16QAM	21	23	30	22	25	26	27	21	21	20
	64QAM	25	28	34	30	28	27	35	32	35	32

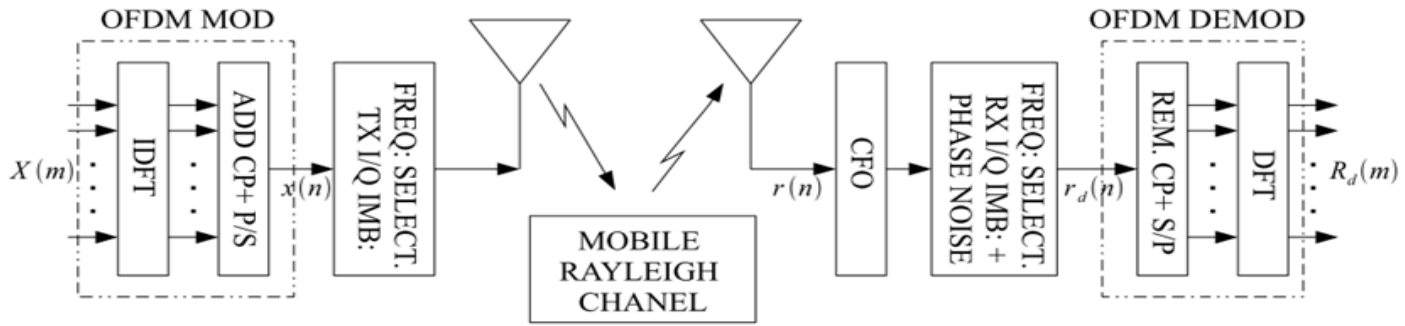


Fig. 1: Block-diagram of the considered system.

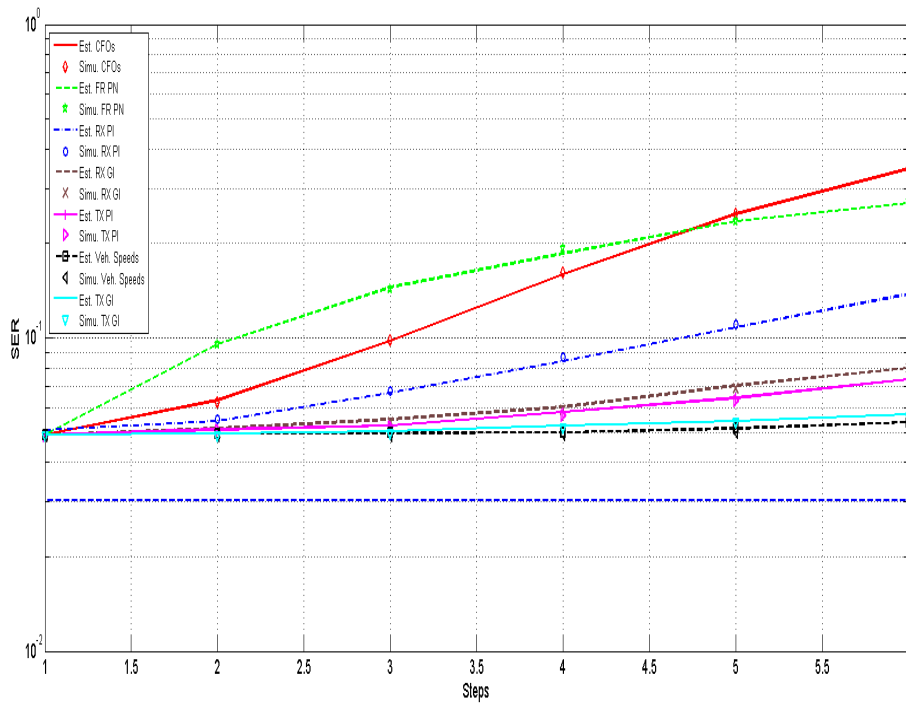
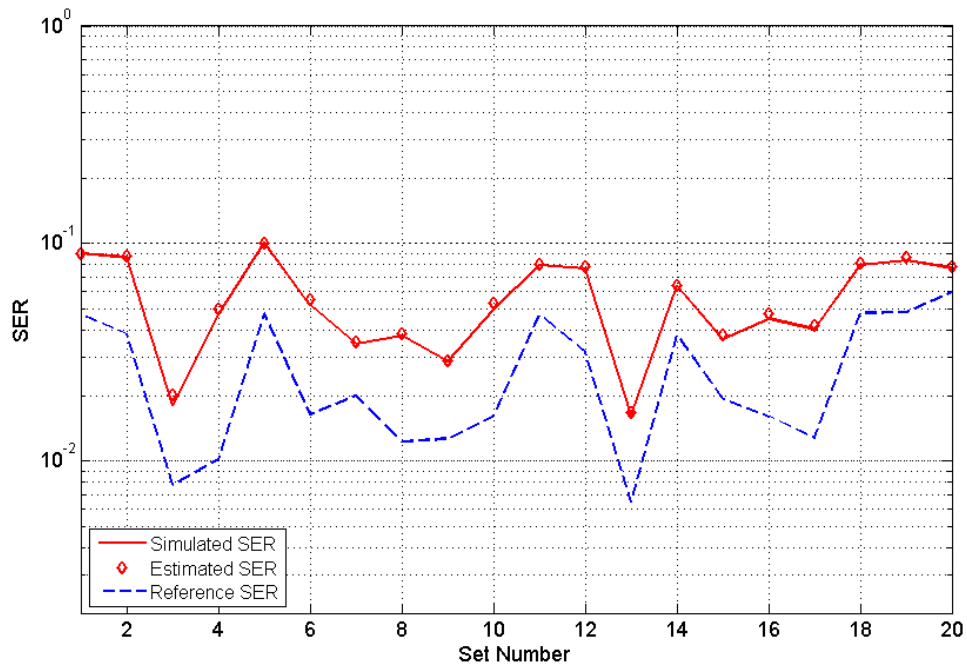
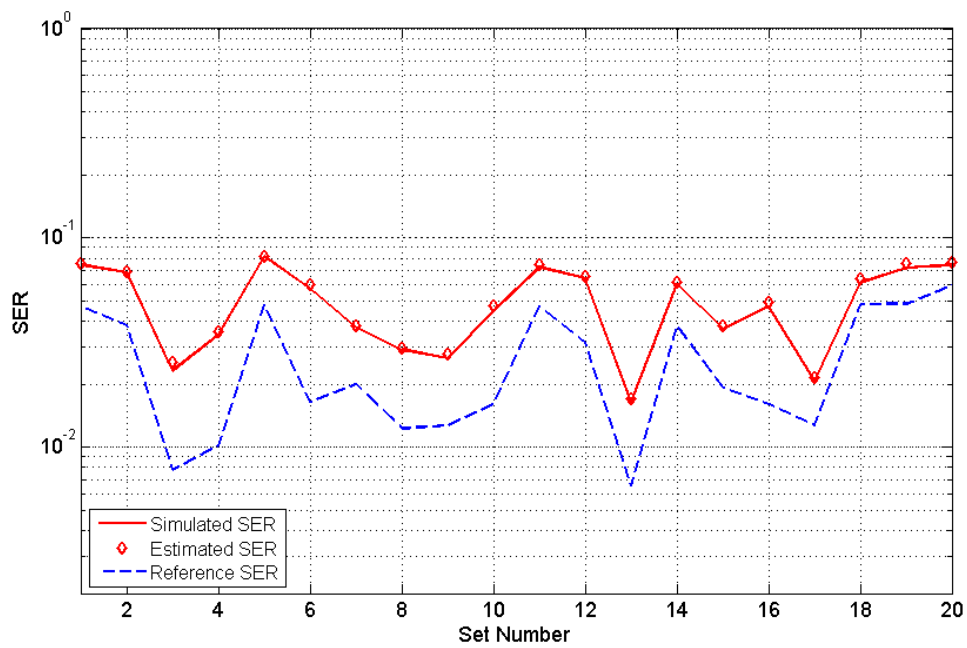


Fig. 2: Comparison of effects of different RF impairments on SER. FR oscillator is implemented.

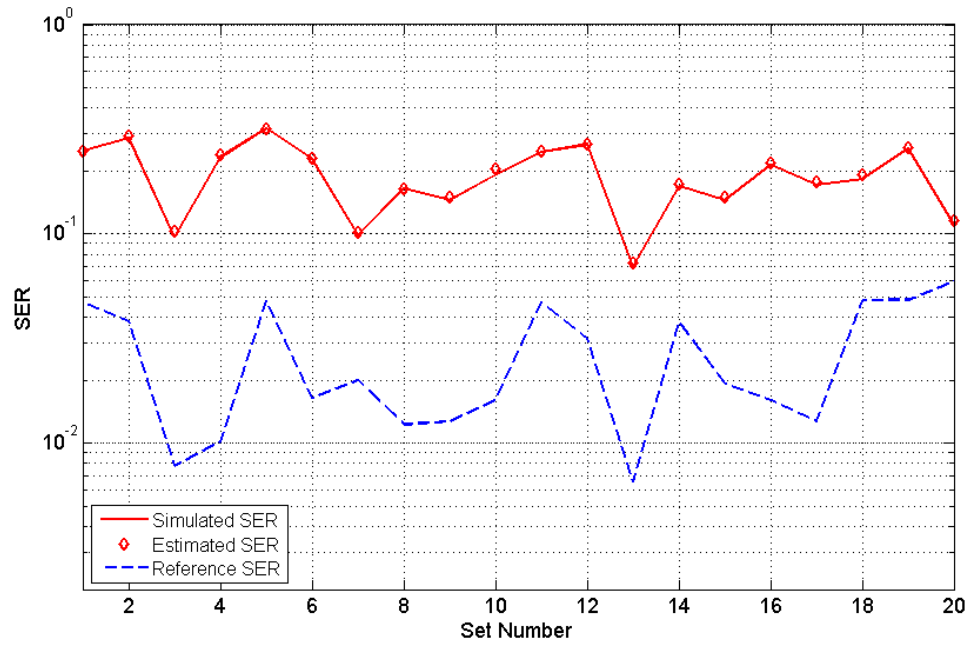


(a) FR oscillator

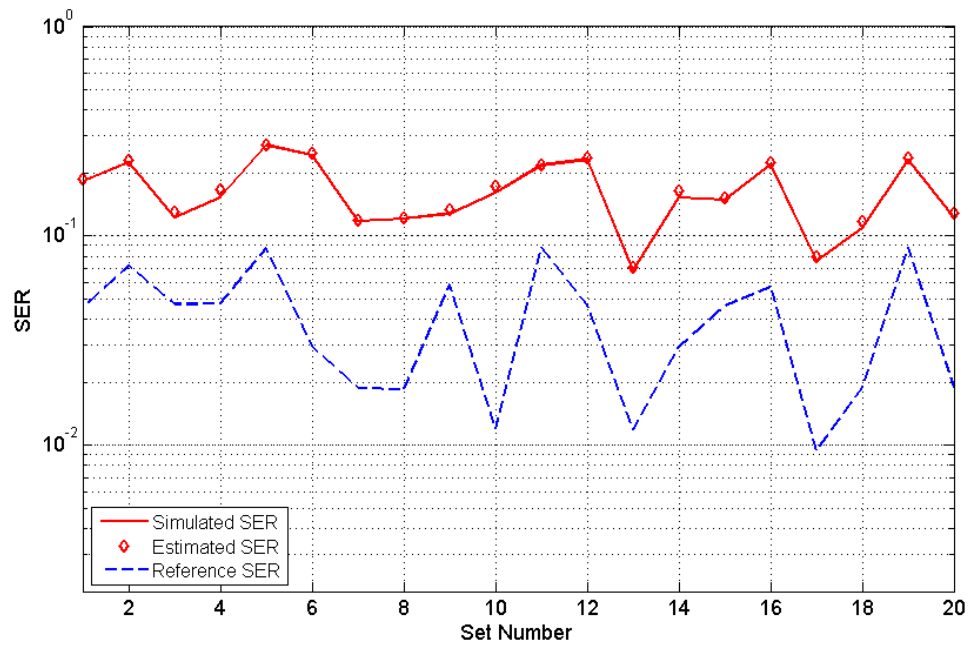


(b) CPPLL oscillator

Fig. 4: Joint effect of multiple RF impairments; 16-QAM. Simulation parameters are given in Tables 2-3.



(a) FR oscillator



(b) CPPLL oscillator

Fig. 5: Joint effect of multiple RF impairments; 64-QAM. Simulation parameters are given in Tables 2-3.

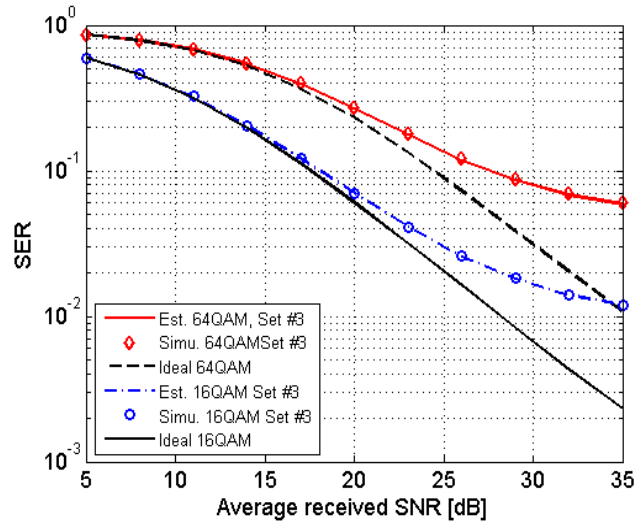


Fig. 6: Comparison of analytical and simulated SER versus received SNR. FR oscillator is implemented.

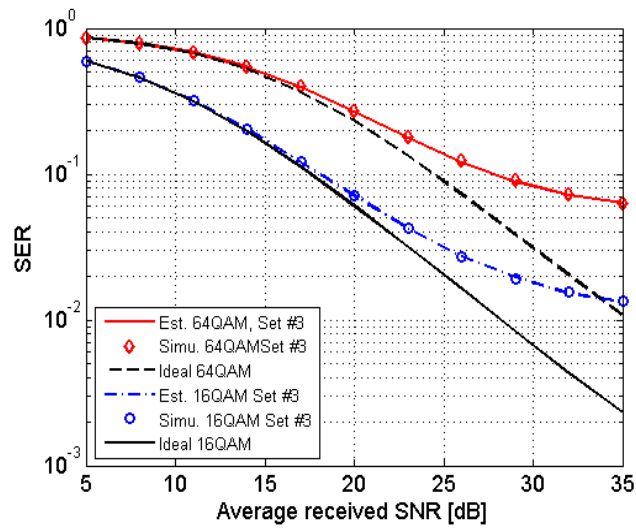


Fig. 7: Comparison of analytical and simulated SER versus received SNR. CPPLL oscillator is implemented.